water

MDPI

Article

Combining Soil Erosion Modeling with Connectivity Analyses to Assess Lateral Fine Sediment Input into Agricultural Streams

Ronald E. Poeppl [1,*], Lina A. Dilly [2], Stefan Haselberger [1], Chris S. Renschler [1,3] and Jantiene E.M. Baartman [2]

[1] Department of Geography and Regional Research, University of Vienna, Universitätsstraße 7, A-1010 Vienna, Austria
[2] Soil Physics and Land Management, Wageningen University, Droevendaalsesteeg 3, 6708PB Wageningen, The Netherlands
[3] Department of Geography, University at Buffalo (SUNY), 116 Wilkeson Quad, Buffalo, NY 14261, USA
* Correspondence: ronald.poeppl@univie.ac.at

Received: 5 July 2019; Accepted: 23 August 2019; Published: 28 August 2019

Abstract: Soil erosion causes severe on- and off-site effects, including loss of organic matter, reductions in soil depth, sedimentation of reservoirs, eutrophication of water bodies, and clogging and smothering of spawning habitats. The involved sediment source-mobilization-delivery process is complex in space and time, depending on a multiplicity of factors that determine lateral sediment connectivity in catchment systems. Shortcomings of soil erosion models and connectivity approaches call for methodical improvement when it comes to assess lateral sediment connectivity in agricultural catchments. This study aims to (i) apply and evaluate different approaches, i.e., Index of Connectivity (IC), the Geospatial Interface for Water Erosion Prediction Project (GeoWEPP) soil erosion model, field mapping and (ii) test a connectivity-adapted version of GeoWEPP (i.e., "GeoWEPP-C") in the context of detecting hot-spots for soil erosion and lateral fine sediment entry points to the drainage network in a medium-sized (138 km^2) agricultural catchment in Austria, further discussing their applicability in sediment management in agricultural catchments. The results revealed that (a) GeoWEPP is able to detect sub-catchments with high amount of soil erosion/sediment yield that represent manageable units in the context of soil erosion research and catchment management; (b) the combination of GeoWEPP modeling and field-based connectivity mapping is suitable for the delineation of lateral (i.e., field to stream) fine sediment connectivity hotspots; (c) the IC is a useful tool for a rapid Geographic Information System (GIS)-based assessment of structural connectivity. However, the IC showed significant limitations for agricultural catchments and functional aspects of connectivity; (d) the process-based GeoWEPP-C model can be seen as a methodical improvement when it comes to the assessment of lateral sediment connectivity in agricultural catchments.

Keywords: water and sediment management; hot-spots; GeoWEPP; index of connectivity (*IC*); sediment dynamics

1. Introduction

Soil erosion has a major impact on the delivery of ecosystem goods and services [1,2], causing severe on- and off-site effects. On-site impacts include loss of organic matter [3,4] and reductions in soil depth [5–7], thus decreasing agricultural productivity [8,9]. Off-site effects are caused by the water-mediated soil export from the fields, resulting in economic damages associated with "muddy flooding" of homes, towns and infrastructure [10,11], and environmental damages, such as eutrophication of water bodies [12–14], clogging and smothering of spawning habitats [15,16],

sedimentation of reservoirs, and the corresponding loss in water storage capacity [17,18]. Effective sediment management on the catchment scale, including the identification of sediment source areas and the way they connect to the channel network, is therefore essential for environmental management [11,19].

The sediment source-mobilization-delivery process is a complex, dynamic continuum [20,21]. Sediment delivery from agricultural landscapes to adjacent watercourses is highly dynamic in space and time, depending on various factors that determine lateral sediment connectivity in fluvial systems [21–23]. These include erosion, transport and deposition processes [24,25], weather events [26], artificial drainage pathways [27–29], land use type, spatial pattern of land use within a watershed, management practices, soil type, and slope [30–34].

While several well-established soil erosion prediction models are available for watersheds (e.g., Soil and Water Assessment Tool (SWAT; [35]), Water Erosion Prediction Project (WEPP; [36]), GeoWEPP (the Geospatial Interface for the process-based soil erosion prediction model WEPP; [37]), the Agricultural Non-Point Source Model (AGNPS; [38]), Sealing and Transfer by Runoff and Erosion related to Agricultural Management (STREAM; [39]), Erosion-3D [40], Limburg Soil Erosion Model (LISEM; [41]), sediment connectivity is still often not described sufficiently, especially in the underlying hydrological catchment models [42,43]. A number of approaches have been used to model sediment delivery to watercourses (e.g., [44–49]; for an overview see [20]). Although much progress has been made over the last two decades, available approaches to model lateral fine sediment connectivity in catchment systems often still do not yield satisfactory results [50,51]; a recent review on indices of sediment connectivity can be found in Heckmann et al. [52]).

In the context of connectivity research, the index of connectivity (*IC*), originally developed by Borselli et al. [53] and elaborated further for various environmental settings (e.g., for alpine catchments by Cavalli et al. [54]; for lowland areas by [55]; for Mediterranean catchments by Gay et al. [56] has become a popular tool to compute sediment connectivity in catchment systems. Compared to process-based models, the *IC* is a static qualitative representation of connectivity in catchment systems [57].

In order to quantify sediment redistribution in catchment systems, some authors have also tried to couple simple physically-based soil erosion models with the *IC* [50,58]. López-Vicente et al. [58], for example, used an enhanced version of the Modified-RMMF (Modified Revised Morgan, [59]; see also [60]) soil erosion model and the *IC* to assess potential soil redistribution for different land use scenarios in a typical Mediterranean agricultural catchment. They found complex spatial patterns in overland flow connectivity and cumulative effective runoff, which were mainly related to changes in topography and land cover. Foerster et al. [43] used the *IC* to assess sediment connectivity in a dryland catchment in the Spanish Pyrenees and reported that connectivity further depends on the spatial distribution of vegetation abundances and small-scale changes in topography. Small-scale changes in land cover and topography have also often been reported to be the major causes for mismatching *IC* results, especially due to quality and resolution of the used input data. In addition, in lowland areas such as valley floors [53,55] runoff and sediment transport processes are strongly influenced by highly dynamic factors such as soil saturation, infiltration capacity, and vegetation growth which are not considered in the *IC*.

The above-mentioned shortcomings of both, soil erosion models and connectivity indices, call for methodical improvement when it comes to assess lateral sediment connectivity in agricultural catchments. Motivated by these challenges, the present study aimed to (i) apply and evaluate different approaches, i.e., *IC*, GeoWEPP, field mapping and (ii) test a connectivity-adapted version of GeoWEPP (i.e., "GeoWEPP-C") in the context of detecting hot-spots for soil erosion (on-site assessment) and lateral fine sediment entry points (connectivity) to the drainage network (off-site assessment), further discussing their applicability in sediment management in agricultural catchments.

2. Study Area

The study is performed in the upper and middle reaches of the Fugnitz catchment that is located in the eastern part of the Bohemian Massif in Lower Austria, next to the Czech Republic border (Figure 1). Within the area of the Thayatal National Park, the Fugnitz River drains into the Thaya River next to the town of Hardegg. The Fugnitz catchment has a total area of 138.4 km^2 and the main stem of the Fugnitz has a length of 29.7 km [30]. The area is characterized by a humid, temperate climate with a mean annual temperature of 8.3 °C and annual precipitation of around 600 mm, with maxima occurring between June and September [30]. The underlying bedrock consists of crystalline mica granite and mica shale [61], which are largely overlain by easily erodible loess layers, marine and fluvial deposits in the upper and middle catchment reaches. Prevalent soil types are different types of Cambisol [62].

The elevation of the catchment ranges between 286.4 and 540.5 m a.s.l. and the topography is characterized by an average slope angle of 2.6° with maximum slope angles up to 32° [30]. The upper parts of the Fugnitz are situated in a relative flat landscape with low river gradients and low slope angles, while the lower reaches are characterized by comparatively steep slopes and V-shaped valleys. This distinct topography in the lower river reaches is a result of vertical incision processes of the Fugnitz River towards the Thaya River. The steeper hillslopes in the upper and middle parts of the catchment are affected by the transport of fine-grained sediments due to water-induced soil erosion. In terms of land use, the upper and middle parts of the catchment are dominated by agricultural areas mainly used for the cultivation of crops (cereals, lucerne, pumpkin, and canola), while the lower parts of the catchment are dominated by forests. Soil tillage is dominated by conventional tillage (i.e., plow or disc tillage after harvest). Sediment and associated nutrient/contaminant input from arable fields to the river channel network of the Fugnitz constitutes one of the major environmental problems for the Thayatal National Park (Figure 2), making it a suitable study area for the purpose of this study.

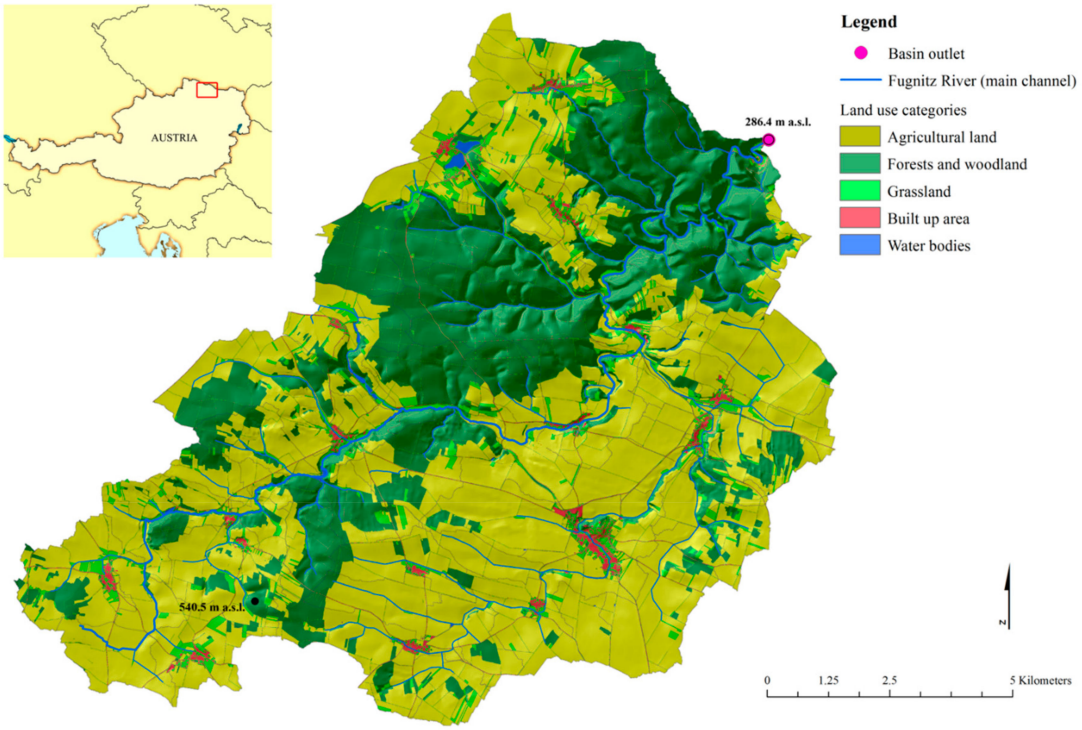

Figure 1. Location and land use of the study area (adapted from Poeppl et al. [30]).

Figure 2. Basin outlet of the Fugnitz River: Sediment-laden Fugnitz River (**A**) draining into the Thaya River (**B**) (photo taken by P. Lazarek in 2009).

3. Methods

This research employs four methods to assess soil erosion and lateral connectivity in the study catchment: soil erosion modeling using GeoWEPP (Section 3.1), computation of the Index of Connectivity (*IC*; Section 3.2), identification of connectivity hotspots in the field (Section 3.3), and application and testing of GeoWEPP-C, which integrates the regular GeoWEPP soil erosion modeling with a connectivity analysis using the contributing area of each cell of the stream (Section 3.4). A flowchart of the various steps taken in this study and their connection is given in Figure 3.

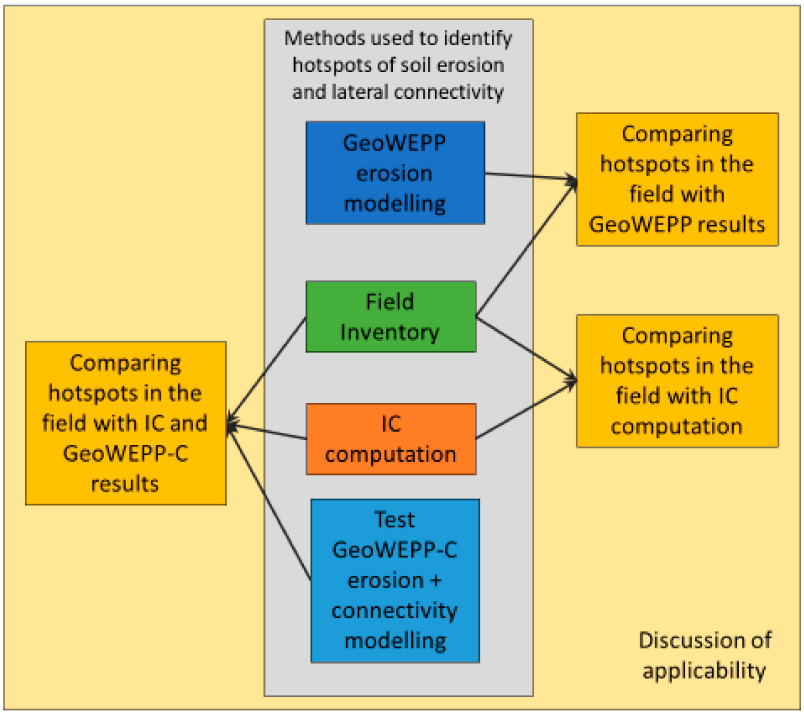

Figure 3. Flowchart of the various methods used and how their results were compared in the study.

3.1. Soil Erosion Modeling (GeoWEPP)

The WEPP soil erosion modeling approach is based on fundamental physical principles and predicts water driven soil erosion either for a single hillslope or a single watershed [36]. It is possible to simulate spatial and temporal distribution of soil loss, sediment yield, and runoff [63]. This approach has been successfully used for different environmental settings [64–69].

GeoWEPP is a stand-alone geospatial interface within the Geographic Information System (GIS) ArcGIS 10.4.1 (ESRI, Redlands, California, USA, 2018) that utilizes the computational power of WEPP for geo-referenced, spatial data analyses, and visualization [37]. The software was developed by the United States Department of Agriculture—Agricultural Research Service (USDA-ARS) and allows the user to import relevant parameters for soil erosion analysis as GIS-layers [70].

In order to run GeoWEPP, a series of datasets was necessary. Information on topography was provided by a Digital Terrain Model (DTM) with 1 m resolution, derived by means of aerial laser scanning (ALS; source: Federal State Government of Lower Austria, 2008). Climate data was obtained from two stations within the catchment (i.e., Geras and Riegersburg; source: Hydrographic Service of Lower Austria, 2017) and included the following parameters: Daily minimum and maximum temperature, daily total, minimum and maximum precipitation, maximum 30-minute rate of precipitation, and maximum 6-hour rate of precipitation; all for the period 1972–2017. The WEPP implemented application CLIGEN—a stochastic weather generator [71]—is able to utilize the monthly-statistics of this detailed 45-year local weather record to generate a 100-years of future storm patterns (storm duration, peak intensity, and time to peak) based on these historic measurements [72]. Soil properties are based on data from the Austrian Federal Office for Water Management (BAW) and included information on soil properties in shapefile format. The shapefile and the corresponding table held information about soil properties for different layers. For each layer, information on soil type, soil moisture, coarser material, humus type and properties, lime content, soil texture and structure, color, root penetration, grain size distribution, pH value, bulk density, and field capacity was available. These data were collected by field measurements and subsequent geostatistical interpolation and inference algorithms in GIS.

The default values for soil albedo, i.e., 0.23 [73], and initial saturation (value for water content in January), i.e., 75%, were used [74]. The cation exchange capacity was set to 0.20 based on the classification by Donahue et al. [75]. The inter-rill and rill erodibility parameter, critical shear stress, and effective hydraulic conductivity of surface soil were calculated by the WEPP model based on the parameter estimation algorithms utilizing the large soils WEPP data base that was derived by nearly a decade of simulated rainfall simulations at numerous locations across the US comparing them to the above-mentioned observations of the soil samples in Austria [36]. Likewise, the information on different land cover types was also provided by the BAW. The 21 classes of the initial file were translated into 7 classes used by the United States Geological Survey (USGS): Open water, bare soil, small grains, low intensity residential, pasture, and mixed forest. Parameters for each land cover class are predefined within GeoWEPP. Information on common management practices was obtained from the Farmers District Division of Hollabrunn, Lower Austria. A frequently used crop rotation concept for a four-year interval (corn–canola–winter wheat–spring wheat) applied in agricultural production in the Fugnitz area was assumed [37]. Additionally, field-derived information on tillage practices (machinery, row width, tillage depth, direction) was used.

As the Fugnitz watershed has an area of roughly 140 km^2 and comprises a large number of sub-catchments and flow paths, model computational power caused some limitations. Hence, the most detailed possible resolution to use for watershed analyses of the whole Fugnitz catchment was 20 m. Therefore, information on topography, soil, and land use had to be resampled. For soil and land use information, a majority resampling approach that determines the value of each pixel based on the predominant value in a 10 m by 10 m window was used. For resampling of the DTM, the mean value of the window was applied. Both adaptations were done with the resampling tool of ArcGIS 10.4.1 (ESRI, Redlands, California, USA, 2018).

Model simulations were executed using the watershed option within the GeoWEPP toolbox in ArcGIS [76]. It identifies a channel network for the watershed and defines hillslopes draining into each channel segment; for each hillslope a representative profile with topographic, soil, and land use information, based on the main influencing parameters for the specific location is created [77]. These representative hillslopes define the various sub-catchments within the model [37]. Instead of using the often-suggested 50 years, a period of 100 years was simulated, as a long simulation period ought to account not only for variations in weather patterns within a particular climate, but also consider the influence of a changing crop rotation with two different crops over a two-year rotation [78].

In June 2017, a rough field-based validation of the GeoWEPP modeling results has been performed using a qualitative mapping approach identifying visible recent soil erosion features using the classification scheme as proposed by Okoba and Sterk [79]. In this study, sheet erosion, rill erosion, and sediment deposition features were mapped in 63 sub-catchments.

3.2. Index of Connectivity (IC) Calculations

The index of connectivity (*IC*), as introduced by Borselli et al. [53], computes sediment connectivity based on topographic information that can be easily derived from a DTM. The *IC* is determined by the ratio between an upslope component referring to the potential for downward routing of sediment produced upslope (Dup, upslope module) and a downslope component (D_{dn}, downslope module) referring to the flow path length that a particle has to travel to the nearest sink or target area (Equation (1)).

$$IC_k = \log_{10}\left(\frac{Dup,k}{Ddn,k}\right) = \log_{10}\left(\frac{\overline{W}_k \overline{S}_k \sqrt{A_k}}{\sum_{i=k,nk} \frac{d_i}{W_i S_i}}\right) \quad (1)$$

where *W* is the average weighting factor of the upslope contributing area *A* (dimensionless and equal to the C-RUSLE factor), *S* is the average slope gradient of the upslope contributing area (m^2), di is the length of the i^{th} cell (dimensionless), and S_i is the slope gradient of the i^{th} cell (m m^{-1}). The subscript *k* indicates that each cell has its own *IC*-value. A schematic overview of the *IC* calculation can be found in Borselli et al. [53].

The *IC* is defined in the range of [−∞, +∞], with larger *IC*-values indicating higher connectivity [53,54]. Numerically speaking, a ratio between the upslope and downslope component equal to one means that a particle upslope potentially has enough energy to travel downslope and reach the target area. Hence, an *IC*-value below 1 indicates that an area is, in terms of sediment connectivity, not connected to the target area. However, empirically, also lower *IC* values around −2 were found to relate to a coupled behavior (Crema, S.; pers. comm., 3 July, 2017). *C*-values (according to the Revised Universal Soil Loss Equation—RUSLE) derived from land use information can be used as a weighting factor in order to model the impedance to runoff and sediment fluxes based on local land use and soil surface properties [53]. Cavalli et al. [54] and Crema et al. [80] adapted the *IC* and developed a software (referred to as SedInConnect) to calculate *IC* values for alpine catchments. Since alpine catchments are dominated by coarse sediment connectivity, SedInConnect, by default, uses surface roughness as weighting factor which is automatically derived from the input DEM. However, using a customized weighting raster is also possible. Furthermore, a distinct target area (of sediment routing) can be defined.

In agricultural catchments, such as the Fugnitz catchment, sediment connectivity is mainly governed by soil erosion processes, being determined by cropping and management practices rather than by coarse scale surface roughness. Therefore, SedInConnect in combination with a customized weighting raster based on *C-values* was used to compute *IC* values for the Fugnitz catchment. Furthermore, since the current research focuses on lateral connectivity the permanent channel network was used as target area for the *IC* computation.

As input data we used the 1 m resolution DTM. To avoid faulty pits in the DTM, the Pit Remove algorithm of TauDEM was used to identify pits and raise their elevation to the level of the lowest pour point around their edge [81]. For the weighting raster, we used *C*-values based on land use data derived from aerial photograph interpretation (see Figure 2; [30]) as weighting factor. As no detailed information was available to determine accurate *C*-values based on crop selection and local circumstances, the current research used average *C*-values similar to those presented in Bakker et al. [82] and Panagos et al. [83] and references mentioned therein (Table 1).

Table 1. *C*-values per land use class used in this study.

Land Use Class.	C-Value
Forest	0.0014
Grassland	0.08
Agricultural land (wheat)	0.2
Built-up area	1×10^{-6}
Riparian zones	0.0014

The computed *IC* values are relative and area specific and a certain *IC* value does not refer to a certain degree of connectivity [53]. To give a relative estimate of the degree of connectivity in the Fugnitz catchment, the computed *IC* values were grouped into 7 connectivity classes (i.e., very low, low, medium low, medium, medium high, high, very high) based on the Jenks natural breaks classification method [84].

3.3. Connectivity Mapping in the Field

Field-based lateral connectivity was assessed by identifying sediment entry points (i.e., sites where sediment enters the permanent channel network) along the main channel of the Fugnitz River (i.e., *IC* target area) based on the mapping method developed by Poeppl et al. [30]. In order to assess the effects of riparian vegetation on lateral sediment connectivity, at each recorded entry point, the vegetated width of the riparian buffer strip was recorded. In addition, as in forested areas soil erosion and related lateral fine sediment input to streams is negligible, further not being the focus of our study, forested areas were not taken into account in the field survey. The survey was carried out in the second week of July 2017.

3.4. Incorporating Connectivity into GeoWEPP: GeoWEPP-C

In contrast to the other process-based catchment models mentioned in Section 1, AgNPS and the Geospatial Interface for WEPP (GeoWEPP; [37]) utilize the topographic parameterization software TOPAZ ([85]) to effectively handle depressions and flat areas in the input DEM using an innovative combination of depression outlet breaching, depression-filling, and relief imposition. TOPAZ generates raster maps and tables that provide properties of contributing hillslope areas to individual channel segments and sub-catchments. In addition, a research version of GeoWEPP for connectivity analysis (i.e., GeoWEPP-C) enables to delineate and simulate representative hillslope contributing areas to individual channel raster cells. This enables to generate a high-resolution mosaic of contributing areas to connectivity points of a drainage network in a landscape (Figure 4).

GeoWEPP-C was tested in a well-connected headwater section of the Fugnitz catchment (see Figure 5), run with a DTM with a 5 m by 5 m resolution for a period of one year (note: In contrast to the 100-year simulation above for sediment yields and watershed outlets, only a 1-year simulation was necessary to identify the potential for the spatial patterns of soil loss; furthermore, there were no crop rotations in the areas with this more detailed assessment), otherwise using the same input data as described in Section 3.1 (GeoWEPP modeling). Computed points with a high potential of lateral sediment connectivity were visually compared with the *IC* results, further being validated by the presence of entry points observed in the field.

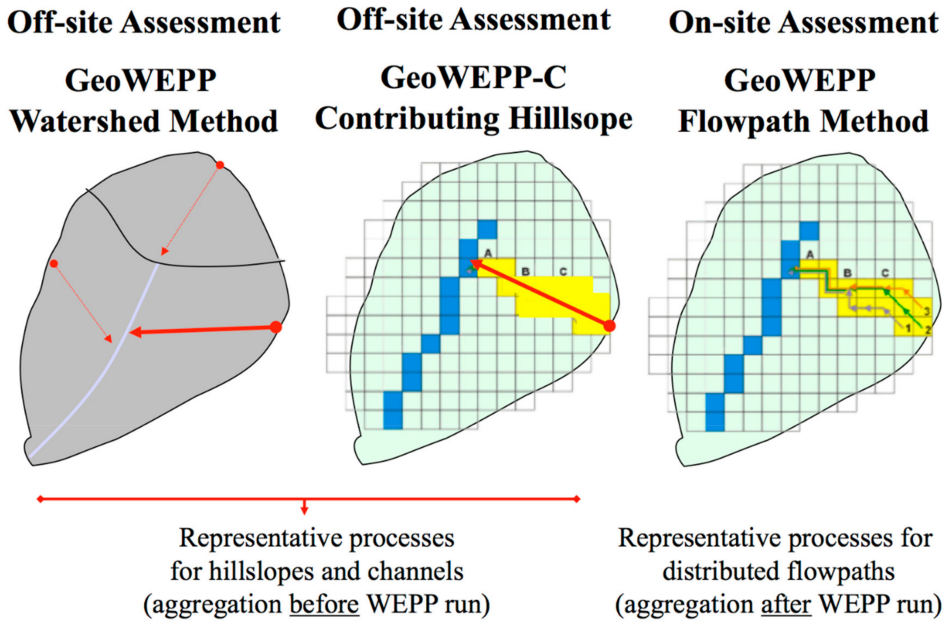

Figure 4. The contributing hillslope to individual channel pixels of a connectivity-adapted version of the Geospatial Interface for Water Erosion Prediction Project (GeoWEPP-C) in comparison to the GeoWEPP watershed and flowpath methods.

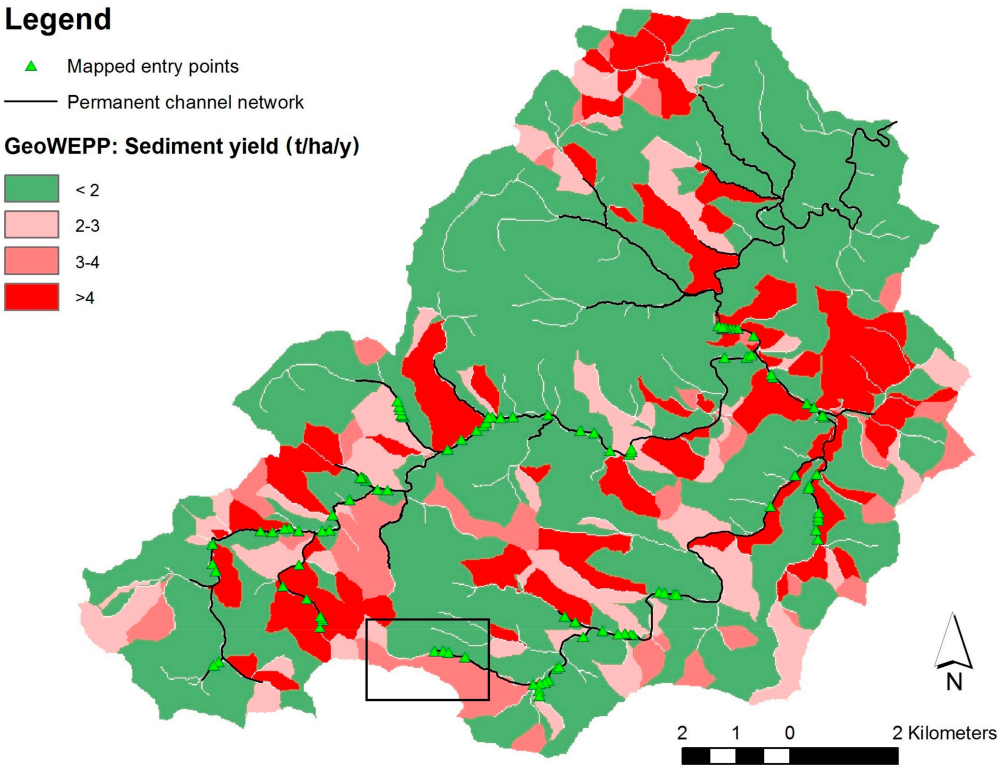

Figure 5. Sediment yield (t/ha/y) as simulated by the GeoWEPP model for a 100-year period. Sediment entry points as found in the field survey are indicated by green triangles (i.e., "mapped entry points"); black rectangle in the southern part of the Fugnitz catchment demarcates the GeoWEPP-C test area (see Section 4.4).

3.5. Inter-Comparison of Methods

First, we compared the *IC* computation with the field findings: In order to validate the general predictive power of the *IC*, rates of mapped entry points were calculated for each *IC* connectivity class. Moreover, example areas were selected to carry out in-depth analyses of the similarities and differences between computed *IC* values and field observations, especially in the context of sediment entry point prediction. Secondly, the GeoWEPP results were compared to the field findings: Potential hotspot areas of fine sediment connectivity were depicted by selecting contributing areas (i.e., areas connected to the channel network by entry points) as computed by GeoWEPP with target values (T) of sediment yield of greater than 2 t/ha/y which lay directly adjacent to the main channel network and these were compared to the location of the mapped entry points. Finally, the GeoWEPP-C results were compared with the *IC* calculations and with the mapped entry points.

4. Results

4.1. Soil Erosion Modeling (GeoWEPP)

Using watershed analyses, predictions on the annual amount of sediment yield per sub-catchment and predictions on runoff for a set of precipitation events for the whole Fugnitz watershed were made. Figure 5 visualizes the catchment wide predictions of sediment yield for a 100-year simulation run. GeoWEPP modeled a total of 731 hillslopes and 295 channels for the Fugnitz watershed. Erosion and sediment yield rates were automatically calculated by GeoWEPP based on a total of 154 storms that produced 567 mm of rainfall on an average annual basis. The model considered a total of 23 high intensity rainfall events with a runoff of 18 mm passing through the watershed outlet on an average annual basis.

As shown in Figure 5, 35% of the modeled sub-catchment areas show increased values of sediment yield (T > 2 t/ha/y), out of which 7% show rates between 3 and 4 t/ha/y, and 17% show the highest amounts of sediment yield (>4 t/ha/y). As mentioned in Section 3.1, WEPP/GeoWEPP estimates low amounts of soil loss and sediment yield for forested areas due to the protective effect of dense vegetation. Therefore, the north-eastern part of the Fugnitz catchment which comprises large areas of forests show less sub-catchments with high values of sediment yield.

During field-based rough qualitative model validation 31 (of 63 sub-catchments) showed indications of soil erosion. 65% of the catchments with visible erosion features showed indications of soil loss due to concentrated flow (rill erosion). Based on the field observations, 22 sub-catchments were rated as having medium to high sediment yields out of which 18 GeoWEPP assigned correctly (a detailed field report can be found in Haselberger 2017 [86]).

4.2. Index of Connectivity (IC) Calculations.

The computed *IC* values for the Fugnitz catchment range from −19.2 to 1.3. The *IC* values were classified into seven connectivity classes (Table 2 and Figure 6). Generally speaking, *IC* values for the Fugnitz catchment are relatively low with an average value of about −11. Only about 0.00013% of the *IC* values are equal or higher to the numerical connectivity threshold value of 1, and 0.32% of the *IC* values are equal or higher than the empirical threshold value of about −2. Agricultural areas close to the channel network (i.e., target area) are usually more connected than areas further away or forested or built-up areas. More distant areas show lower *IC*-values due to the longer flow path lengths that a particle has to travel. Nonetheless, there are also areas close to the channel network being rather disconnected according to their *IC*-values, as the *IC* also depends on the potential for downward routing of sediment and the weighting raster.

Table 2. Index of connectivity (*IC*) classification based on the Jenks natural breaks classification method.

Connectivity	*IC*-Values
Very low	$-19.21 \leq IC < -15.00$
Low	$-15.00 \leq IC < -13.00$
Medium low	$-13.00 \leq IC < -11.50$
Medium	$-11.50 \leq IC < -10.00$
Medium high	$-10.00 \leq IC < -8.50$
High	$-8.50 \leq IC < -7.00$
Very high	$-7.00 \leq IC \leq 1.32$

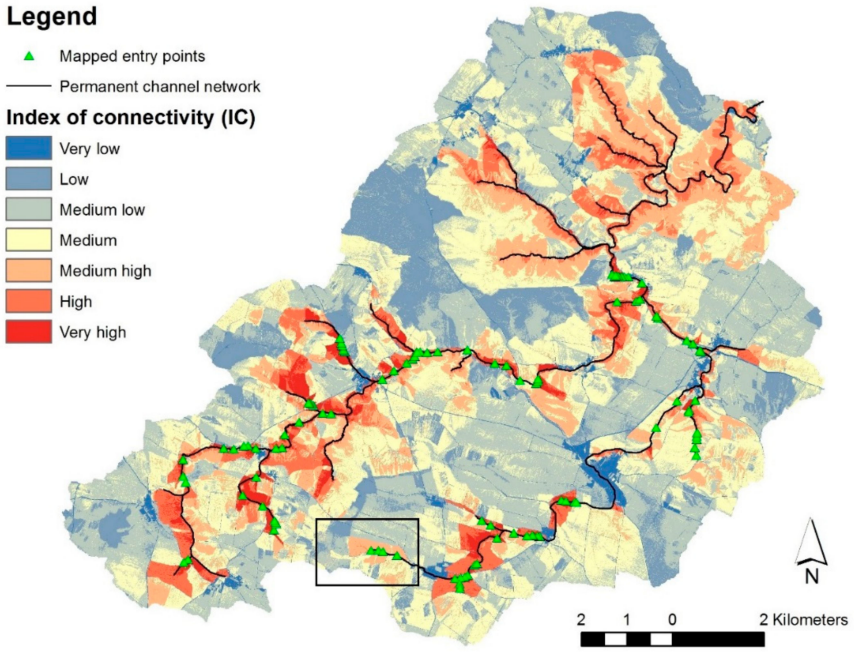

Figure 6. Classified computed *IC* values for the Fugnitz catchment. Sediment entry points as found in the field survey are indicated by green triangles (i.e., "mapped entry points"); black rectangle in the southern part of the Fugnitz catchment demarcates the GeoWEPP-C test area (see Section 4.4).

4.3. Connectivity Mapping, IC Validation, and Hot-Spot Delineation

A total of 107 sediment entry points were identified in the field (Figure 7; see also Figures 5 and 6), resulting in hotspot areas occupying 6.19 km^2 (4.47%) of the total Fugnitz catchment area. Most sediment entry points were found in areas with no or relatively narrow riparian vegetation of max. 2.5 m (Table 3). Approximately one third of the sediment entry points are located in areas with riparian buffer strips of three meters and more. The majority (85%) of the sediment entry points is located in areas that are classified as very highly or highly connected based on their *IC*-values (Table 4). However, in the context of sediment entry point prediction, in-depth analyses of the similarities and differences between computed *IC* values and field observations (i.e., sediment entry points) have shown discrepancies between predicted and observed entry points.

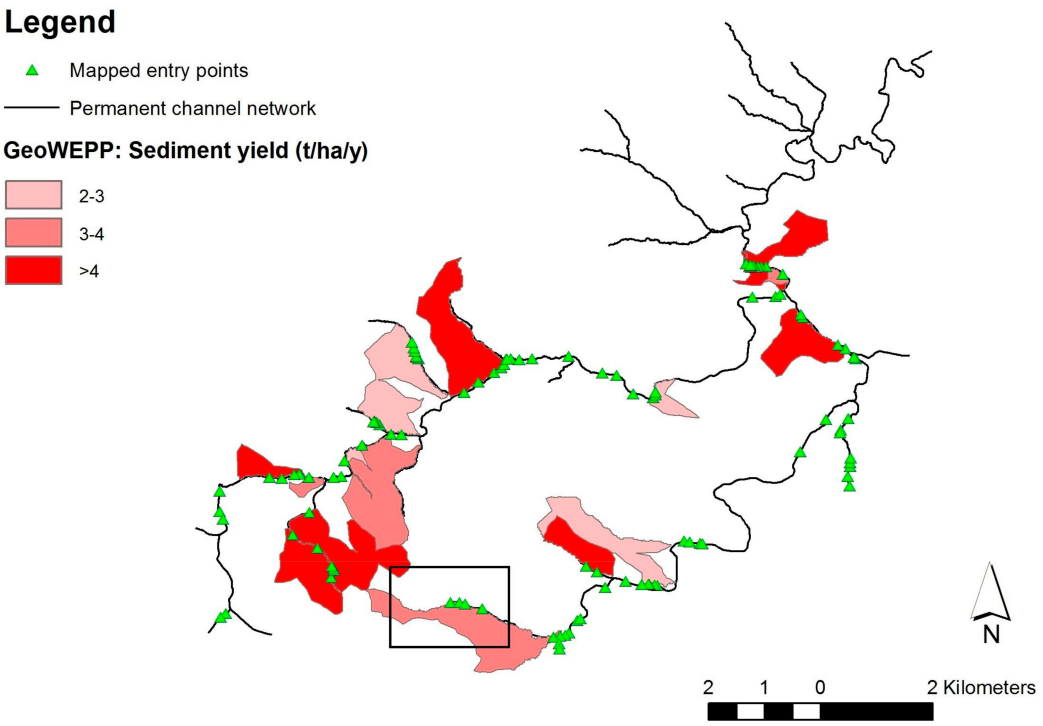

Figure 7. Hotspots for lateral fine sediment yields (t/ha/yr) as inputs based on GeoWEPP modeling and connectivity mapping; black rectangle in the southern part of the Fugnitz catchment demarcates the GeoWEPP-C test area (see Section 4.4).

Table 3. Riparian vegetation near sediment entry points. The table shows the percentage of sediment entry points for different riparian buffer strip widths (m).

Width of Buffer Strip (m)	Entry Points (%)
0	17
0.5–2.5	45
3–5	34
>5	4

Table 4. Distribution of the mapped sediment entry points over the different *IC* classes (see also Table 2).

IC Class	Entry Points (%)
Very low	0
Low	1
Medium low	3
Medium	4
Medium high	7
High	21
Very high	64

4.4. GeoWEPP-C Results for the Test Area

GeoWEPP-C modeling results for the test area are shown in Figure 8b,c. Figure 8b shows the on-site soil loss of the contributing hillslopes in the test area (i.e., on-site assessment), while the calculated sediment yields of representative hillslopes for individual channel pixel (i.e., off-site assessment results) are shown in Figure 8c.

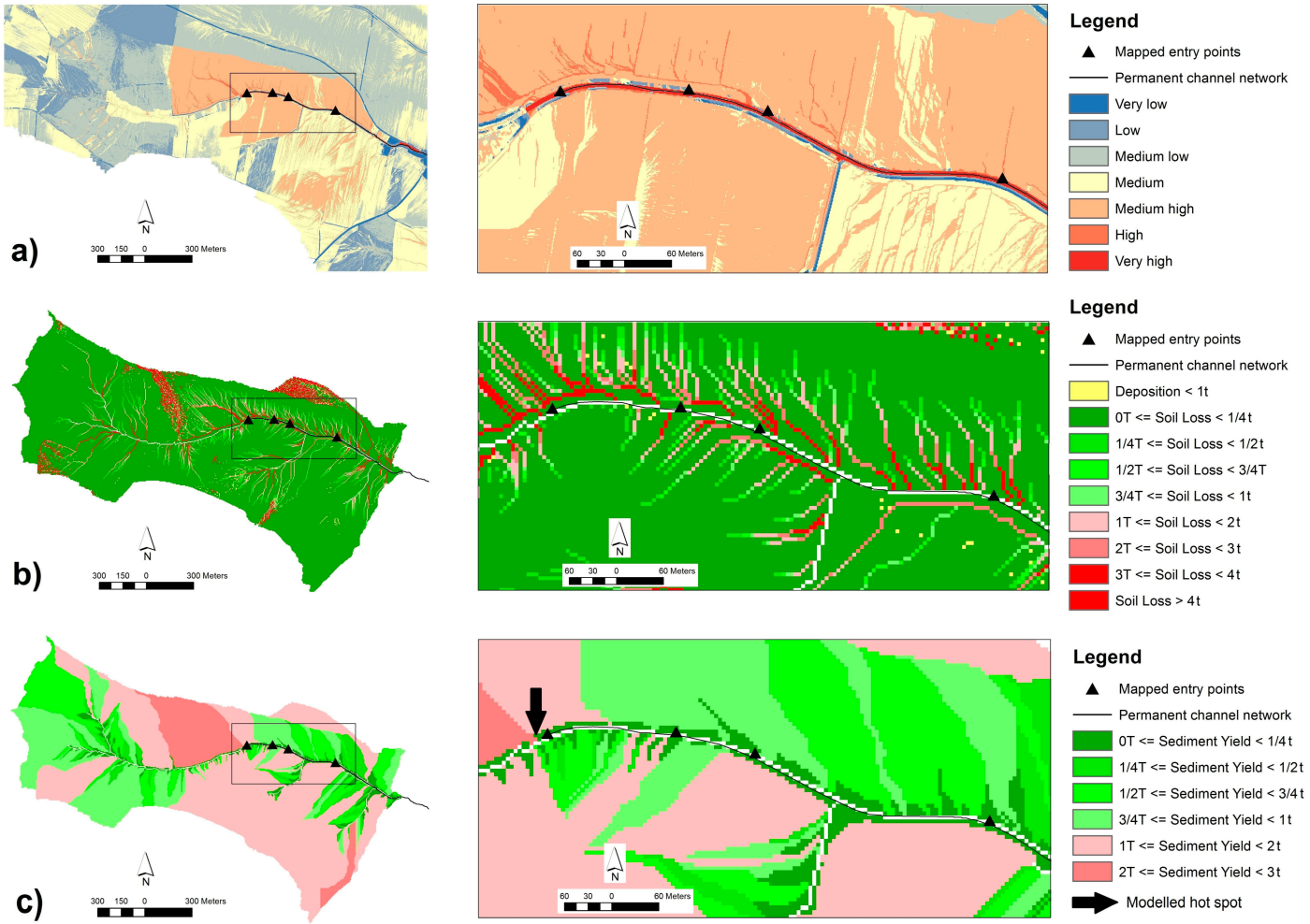

Figure 8. GeoWEPP-C modeling results for the test area (1 y simulation period; target value T = 2 t/ha/yr) illustrating a comparison between the three methodologies illustrating hotspots of connectivity, soil losses, and sediment yields: (**a**) *IC*-results for comparison (see also Figure 6); (**b**) GeoWEPP visualization of soil loss along flowpaths towards river channels (on-site assessment); (**c**) GeoWEPP-C visualization of sediment yields of contributing areas into individual channel pixels (off-site assessment). Note: All mapped entry points are located at the north banks of the river channel.

GeoWEPP-C soil loss modeling results (see Figure 8b) show a high number (n = 14) of highly productive (>3t/ha/y of soil loss) flowpaths, exhibiting a north-bank connection to the river channel (i.e., location of mapped entry points). In contrast, the *IC* calculations resulted in a low number (n = 5) of connected flowpaths with high connectivity values. None of the potential entry points calculated by GeoWEPP-C, and one flowpath exhibiting high *IC* values, showed a perfect match to the entry points observed in the field.

GeoWEPP-C sediment yield modeling results (see Figure 8c, left) show highly diverse patterns of sediment contributing areas reflecting areas of different lateral sediment connectivity potential. Three (out of four) of the mapped entry points were observed to be located adjacent to modeled entry points of contributing areas with sediment yield values of <1 t/ha/y, while one (i.e., the most western) entry point is located adjacent to modeled entry points of contributing areas with sediment yield values of >2 t/ha/y (i.e., modeled lateral fine sediment connectivity hotspot; see Figure 8c, right). However, it should be kept in mind that a discrepancy between the modeled output and the mapped sediment entry point may also be due to GPS (in)accuracy in the field.

5. Discussion

5.1. Soil Erosion Modeling (GeoWEPP)

The predicted amounts of soil loss are in line with measured values from Lower Austria. Klik [87], for example, investigated a small agriculturally used catchment in Mistelbach, Lower Austria, and reported soil loss rates between 0 and 11.59 t/ha/y. Values for the Fugnitz catchment calculated by GeoWEPP ranged between 0.28 and 11.7 t/ha/y.

It was possible to run the GeoWEPP watershed application for the whole Fugnitz catchment and to simulate the spatial distribution of sediment yield for a period of 100 years using an input DEM with 20 m by 20 m resolution. A major challenge for assessing soil erosion hotspots in medium-sized or large catchment systems is the quality/spatial resolution of the input data. As it is often difficult to obtain data with a high spatial and temporal resolution for larger catchments, generalization is necessary and various parameters that influence soil erosion processes may not be covered [88,89].

According to the main objective of this study, GeoWEPP was able to highlight areas of interest (i.e., sub-catchments with high amount of soil erosion/sediment yield), representing fundamental/manageable units of study [90] in the context of soil erosion research and catchment management. Moreover, combining GeoWEPP modeling of on-site soil loss for hillslopes and off-site sediment yields into channels (see also comment in Figure 8 caption) with field-based connectivity mapping has shown to be a suitable approach for the delineation of lateral fine sediment connectivity hotspots. Like other soil erosion models (e.g., SWAT; e.g., [91]), GeoWEPP can also be used for site-specific future soil and water conservation planning and management under different climate, land cover, and management/conservation scenarios [36,37,63,92].

5.2. Index of Connectivity (IC)

The calculation of *IC*-values requires detailed and high-resolution input data based on catchment-specific factors influencing connectivity, such as topography and land cover characteristics. Like already observed in other studies, the discrepancies between the computed *IC* results and field observations suggest that fine sediment connectivity in agricultural catchments is not mainly topography driven but depends on other (process-based) factors including infiltration and runoff [55,93,94]. Furthermore, the DEM, which was used for the *IC* calculations, did not take pipes and culverts into account, potentially leading to errors in the flow pathway calculations. To reduce this impact, the course of the stream network was partially manually corrected. However, a completely revised DTM could considerably increase the validity of the *IC* computation [94].

Choosing the permanent channel network as target has led to generally low *IC* values, due to large distances between remote catchment areas to the permanent channels. However, during large storms

or wet periods, also periodic streams might become active and connected, increasing connectivity, further emphasizing the dynamic component of connectivity (cf. [21]). In the context of the study aims, the *IC* has shown to be suitable for rapid GIS-based assessments of structural connectivity, with some significant limitations for agricultural catchments, mainly related (but not limited) to lacking information on functional (i.e., process-related dynamic) aspects of connectivity.

5.3. GeoWEPP-C

The process-based GeoWEPP-C model has shown to be capable of simultaneously computing flowpaths towards channels (i.e., potential entry points; on-site assessment) and sediment yields of contributing areas into individual channel pixels (off-site assessment). Due to a high processing demand of GeoWEPP-C, it was only possible to run it for a test area with spatial resolution of minimum 5 m by 5 m. Compared to the *IC*, GeoWEPP-C modeled a high number of flowpaths with a high connectivity potential. It was also possible to use GeoWEPP-C to compute sediment yields of contributing areas into individual channel pixels, thereby being able to delineate hotspots for lateral fine sediment input to agricultural streams.

In the context of soil erosion modeling and sediment connectivity research, the process-based GeoWEPP-C model can be seen a methodical improvement when it comes to assess lateral sediment connectivity in agricultural catchments. Nevertheless, it has to be stated that GeoWEPP-C at this point is still in an experimental stage, not being ready for practical application, especially due to increased computational demand with high resolution DEMs. Moreover, the model needs to be tested in different environmental settings, and in the light of its applicability in the context of catchment management (incl. climate and land use change scenario modeling).

6. Conclusions

This study applied various approaches to detect hotspots of soil erosion and lateral fine sediment input to the drainage network. The methods applied include the Index of Connectivity (*IC*), GeoWEPP erosion modeling, field mapping and testing the connectivity-adapted version of GeoWEPP called GeoWEPP-C. The results of the various methods were inter-compared and discussed in terms of their applicability in sediment management in agricultural catchments. Based on the obtained results the following conclusions can be drawn:

- GeoWEPP is able to detect sub-catchments with high amount of soil erosion/sediment yield that represent manageable units in the context of soil erosion research and catchment management;
- Combining GeoWEPP modeling with field-based connectivity mapping has shown to be suitable for the delineation of lateral fine sediment connectivity hotspots;
- The *IC* is a useful tool for a quick GIS-based assessment of structural connectivity, however showing significant limitations for agricultural catchments which are mainly related (but not limited) to lacking information on functional aspects of connectivity;
- The process-based GeoWEPP-C model can be seen a methodical improvement when it comes to assess lateral sediment connectivity in agricultural catchments. However, the model needs some more improvement, especially for the high computational demanding use of the ever-increasing higher spatial resolution before it is ready for practical application (e.g., in the contexts of soil erosion and surface water management).

Author Contributions: Conceptualization: R.E.P.; Methodology: R.E.P., L.A.D., S.H., C.S.R., J.E.M.B.; Software (GeoWEPP): C.S.R.; Validation: L.A.D., S.H.; Formal analysis: R.E.P., L.A.D., S.H., C.S.R., J.E.M.B.; Investigation: L.A.D., S.H., and C.S.R.; writing—original draft preparation: R.E.P.; Writing—review and editing: R.E.P.

Funding: This research received no external funding.

Acknowledgments: The authors are thankful for the support given by the Thayatal National Park authority.

Conflicts of Interest: The authors declare no conflict of interest.

References

1. Graves, A.; Morris, J.; Deeks, L.; Rickson, J.; Kibblewhite, M.; Harris, J.; Farewell, T. The Total Costs of Soils Degradation in England and Wales. *Ecol. Econ.* **2015**, *119*, 399–413. [CrossRef]
2. Lal, R. Soil erosion by wind and water: Problems and prospects. In *Soil Erosion Research Methods*; Routledge: New York, NY, USA, 1994; pp. 1–10.
3. Pimentel, D. Soil erosion: A food and environmental threat. *Environ. Dev. Sustain.* **2006**, *8*, 119–137. [CrossRef]
4. Glendell, M.; Brazier, R. Accelerated export of sediment and carbon from a landscape under intensive agriculture. *Sci. Total Environ.* **2014**, *476*, 643–656. [CrossRef] [PubMed]
5. Pimentel, D.; Harvey, C.; Resosudarmo, P.; Sinclair, K.; Kurz, D.; McNair, M.; Crist, S.; Shpritz, L.; Fitton, L.; Saffouri, R.; et al. Environmental and economic costs of soil erosion and conservation benefits. *Sci.-Aaas-Wkly. Pap. Ed.* **1995**, *267*, 1117–1122. [CrossRef] [PubMed]
6. Wardle, D.A.; Bardgett, R.D.; Klironomos, J.N.; Setala, H.; Putten, W.H.; Wall, D.H. Ecological linkages between aboveground and belowground biota. *Science* **2004**, *304*, 1629–1633. [CrossRef] [PubMed]
7. Lal, R. Soil conservation and ecosystem services. *Int. Soil Water Conserv. Res.* **2014**, *2*, 36–47. [CrossRef]
8. Mullan, D. Soil erosion under the impacts of future climate change: Assessing the statistical significance of future changes and the potential on-site and off-site problems. *Catena* **2013**, *109*, 234–246. [CrossRef]
9. Panagos, P.; Standardi, G.; Borrelli, P.; Lugato, E.; Montanarella, L.; Bosello, F. Cost of agricultural productivity loss due to soil erosion in the European Union: From direct cost evaluation approaches to the use of macroeconomic models. *Land Degrad. Dev.* **2018**, *29*, 471–484. [CrossRef]
10. Boardman, J. A short history of muddy floods. *Land Degrad. Dev.* **2010**, *21*, 303–309. [CrossRef]
11. Boardman, J.; Vandaele, K.; Evans, R.; Foster, I.D.L. Off-site impacts of soil erosion and runoff: Why connectivity is more important than erosion rates. *Soil Use Manag.* **2019**, *35*, 245–256. [CrossRef]
12. Jarvie, H.P.; Neal, C.; Withers, P.J.A. Sewage-effluent phosphorus: A greater risk to river eutrophication than agricultural phosphorus? *Sci. Total Environ.* **2006**, *360*, 246–253. [CrossRef] [PubMed]
13. Issaka, S.; Ashraf, M.A. Impact of soil erosion and degradation on water quality: A review. *Geol. Ecol. Landsc.* **2017**, *1*, 1–11. [CrossRef]
14. Nadal-Romero, E.; Khorchani, M.; Lasanta, T.; García-Ruiz, J.M. Runoff and Solute Outputs under Different Land Uses: Long-Term Results from a Mediterranean Mountain Experimental Station. *Water* **2019**, *11*, 976. [CrossRef]
15. Walling, D.E.; Amos, C.M. Source, storage and mobilisation of fine sediment in a chalk stream system. *Hydrol. Process.* **1999**, *13*, 323–340. [CrossRef]
16. Denic, M.; Geist, J. Linking stream sediment deposition and aquatic habitat quality in pearl mussel streams: Implications for conservation. *River Res. Appl.* **2015**, *31*, 943–952. [CrossRef]
17. Verstraeten, G.; Bazzoffi, P.; Lajczak, A.; Radoane, M.; Rey, F.; Poesen, J.; de Vente, J. Reservoir and pond sedimentation in Europe. In *Soil Erosion in Europe*; Boardman, J., Poesen, J., Eds.; Wiley: Chichester, UK, 2006; pp. 757–774.
18. Schleiss, A.J.; Franca, M.J.; Juez, C.; De Cesare, G. Reservoir sedimentation. *J. Hydraul. Res.* **2016**, *54*, 595–614. [CrossRef]
19. Reid, S.C.; Lane, S.N.; Montgomery, D.R.; Brookes, C.J. Does hydrological connectivity improve modelling of coarse sediment delivery in upland environments? *Geomorphology* **2007**, *90*, 263–282. [CrossRef]
20. Rickson, R.J. Can control of soil erosion mitigate water pollution by sediments? *Sci. Total Environ.* **2014**, *468*, 1187–1197. [CrossRef]
21. Bracken, L.J.; Turnbull, L.; Wainwright, J.; Bogaart, P. Sediment connectivity: A framework for understanding sediment transfer at multiple scales. *Earth Surf. Process. Landf.* **2015**, *40*, 177–188. [CrossRef]
22. Bracken, L.J.; Croke, J. The concept of hydrological connectivity and its contribution to understanding runoff dominated geomorphic systems. *Hydrol. Process.* **2007**, *21*, 17491763. [CrossRef]
23. Poeppl, R.E.; Keesstra, S.D.; Maroulis, J. A conceptual connectivity framework for understanding geomorphic change in human-impacted fluvial systems. *Geomorphology* **2017**, *277*, 237–250. [CrossRef]
24. Parsons, A.; Wainwright, J.; Powell, D.; Kaduk, J.; Brazier, R. A conceptual model for determining soil erosion by water. *Earth Surf. Process. Landf.* **2004**, *29*, 1293–1302. [CrossRef]

25. Govers, G. Misapplications and misconceptions of erosion models. In *Handbook of Erosion Modelling*; Morgan, R.P.C., Nearing, M.A., Eds.; Wiley-Blackwell: Chichester, UK, 2011; pp. 117–134.
26. Reaney, S.M.; Bracken, L.J.; Kirkby, M.J. The importance of surface controls on overland flow connectivity in semi-arid environments: Results from a numerical experimental approach. *Hydrol. Process.* **2014**, *28*, 2116–2128. [CrossRef]
27. Newson, M.D. The erosion of drainage ditches and its effect on bedload yields in mid-Wales: Reconnaissance studies. *Earth Surf. Process. Landf.* **1980**, *5*, 275–290. [CrossRef]
28. Hösl, R.; Strauss, P.; Glade, T. Man-made linear flow paths at catchment scale: Identification, factors and consequences for the efficiency of vegetated filter strips. *Landsc. Urban Plan.* **2012**, *104*, 245–252. [CrossRef]
29. Calsamiglia, A.; Garcia-Comendador, J.; Fortesa, J.; López-Tarazón, J.A.; Crema, S.; Cavalli, M.; Calvo-Cases, A.; Estrany, J. Effects of agricultural drainage systems on sediment connectivity in a small Mediterranean lowland catchment. *Geomorphology* **2018**, *318*, 162–171. [CrossRef]
30. Poeppl, R.E.; Keiler, M.; Elverfeldt, K.v.; Zweimueller, I.; Glade, T. The influence of riparian vegetation cover on diffuse lateral connectivity and biogeomorphic processes in a medium-sized agricultural catchment, Austria. *Geogr. Ann. Ser. A* **2012**, *94*, 511–529. [CrossRef]
31. Koiter, A.J.; Owens, P.N.; Petticrew, E.L.; Lobb, D.A. The behavioural characteristics of sediment properties and their implications for sediment fingerprinting as an approach for identifying sediment sources in river basins. *Earth Sci. Rev.* **2013**, *125*, 24–42. [CrossRef]
32. Lamba, J.; Karthikeyan, K.G.; Thompson, A.M. Apportionment of suspended sediment sources in an agricultural watershed using sediment fingerprinting. *Geoderma* **2015**, *239*, 25–33. [CrossRef]
33. Keesstra, S.; Nunes, J.P.; Saco, P.; Parsons, T.; Poeppl, R.; Masselink, R.; Cerdà, A. The way forward: Can connectivity be useful to design better measuring and modelling schemes for water and sediment dynamics? *Sci. Total Environ.* **2018**, *644*, 1557–1572. [CrossRef]
34. Choi, K.; Maharjan, G.R.; Reineking, B. Evaluating the Effectiveness of Spatially Reconfiguring Erosion Hot Spots to Reduce Stream Sediment Load in an Upland Agricultural Catchment of South Korea. *Water* **2019**, *11*, 957. [CrossRef]
35. Arnold, J.G.; Fohrer, N. SWAT2000: Current capabilities and research opportunities in applied watershed modelling. *Hydrol. Process.* **2005**, *19*, 563–572. [CrossRef]
36. Flanagan, D.C.; Nearing, M.A. *USDA-Water Erosion Prediction Project: Hillslope Profile and Watershed Model Documentation*; NSERL Report; USDA-ARS National Soil Erosion Research Laboratory: West Lafayette, IN, USA, 1995; Volume 10, pp. 1603–1612.
37. Renschler, C.S. Designing geo-spatial interfaces to scale process models: The GeoWEPP approach. *Hydrol. Process.* **2003**, *17*, 1005–1017. [CrossRef]
38. Young, R.A.; Onstad, C.A.; Bosch, D.D.; Anderson, W.P. AGNPS: A nonpoint-source pollution model for evaluating agricultural watersheds. *J. Soil Water Conserv.* **1989**, *44*, 168–173.
39. Cerdan, O.; Souchère, V.; Lecomte, V.; Couturier, A.; Le Bissonnais, Y. Incorporating soil surface crusting processes in an expert-based runoff model: Sealing and transfer by runoff and erosion related to agricultural management. *Catena* **2002**, *46*, 189–205. [CrossRef]
40. Schmidt, J. A mathematical model to simulate rainfall erosion. *Catena* **1991**, *19*, 101–109.
41. De Roo, A.P.J.; Wesseling, C.G.; Ritsema, C.J. LISEM: A single-event physically based hydrological and soil erosion model for drainage basins. I: Theory, input and output. *Hydrol. Process.* **1996**, *10*, 1107–1117. [CrossRef]
42. De Vente, J.; Poesen, J.; Bazzoffi, P.; Rompaey, A.V.; Verstraeten, G. Predicting catchment sediment yield in Mediterranean environments: The importance of sediment sources and connectivity in Italian drainage basins. *Earth Surf. Process. Landf.* **2006**, *31*, 1017–1034. [CrossRef]
43. Foerster, S.; Wilczok, C.; Brosinsky, A.; Segl, K. Assessment of sediment connectivity from vegetation cover and topography using remotely sensed data in a dryland catchment in the Spanish Pyrenees. *J. Soils Sediments* **2014**, *14*, 1982–2000. [CrossRef]
44. Johnes, P.J. Evaluation and management of the impact of land-use change on the nitrogen and phosphorus load delivered to surface waters: The export coefficient modelling approach. *J. Hydrol.* **1996**, *183*, 323–349. [CrossRef]
45. Haygarth, P.M.; Jarvis, S.C. Transfer of phosphorus from agricultural soil. *Adv. Agron.* **1999**, *66*, 195–249.

46. Heathwaite, A.L.; Fraser, A.I.; Johnes, P.J.; Hutchins, M.; Lord, E.; Butterfield, D. The Phosphorus Indicators Tool: A simple model of diffuse P Loss from agricultural land to water. *Soil Use Manag.* **2003**, *19*, 1–11. [CrossRef]
47. Davison, P.S.; Withers, P.J.; Lord, E.I.; Betson, M.J.; Strömqvist, J. PSYCHIC–A process-based model of phosphorus and sediment mobilisation and delivery within agricultural catchments. Part 1: Model description and parameterisation. *J. Hydrol.* **2008**, *350*, 290–302. [CrossRef]
48. Gumiere, S.J.; Le Bissonnais, Y.; Raclot, D.; Cheviron, B. Vegetated filter effects on sedimentological connectivity of agricultural catchments in erosion modelling: A review. *Earth Surf. Process. Landf.* **2011**, *36*, 3–19. [CrossRef]
49. Jetten, V.G.; Maneta, M.P. Calibration of erosion models. In *Handbook of Erosion Modelling*; Morgan, R.P.C., Nearing, M.A., Eds.; Wiley-Blackwell: Chichester, UK, 2011; pp. 33–51.
50. López-Vicente, M.; Quijano, L.; Palazón, L.; Gaspar, L.; Izquierdo, A.N. Assessment of soil redistribution at catchment scale by coupling a soil erosion model and a sediment connectivity index (Central Spanish Pre-Pyrenees). *Cuad. Investig. Geográfica/Geogr. Res. Lett.* **2015**, *41*, 127–147. [CrossRef]
51. López-Vicente, M.; Ben-Salem, N. Computing structural and functional flow and sediment connectivity with a new aggregated index: A case study in a large Mediterranean catchment. *Sci. Total Environ.* **2019**, *651*, 179–191. [CrossRef]
52. Heckmann, T.; Cavalli, M.; Cerdan, O.; Foerster, S.; Javaux, M.; Lode, E.; Smetanová, A.; Vericat, D.; Brardinoni, F. Indices of sediment connectivity: Opportunities, challenges and limitations. *Earth-Sci. Rev.* **2018**, *187*, 77–108. [CrossRef]
53. Borselli, L.; Cassi, P.; Torri, D. Prolegomena to sediment and flow connectivity in the landscape: A GIS and field numerical assessment. *Catena* **2008**, *75*, 268–277. [CrossRef]
54. Cavalli, M.; Trevisani, S.; Comiti, F.; Marchi, L. Geomorphometric assessment of spatial sediment connectivity in small Alpine catchments. *Geomorphology* **2013**, *188*, 31–41. [CrossRef]
55. Gay, A.; Cerdan, O.; Mardhel, V.; Desmet, M. Application of an index of sediment connectivity in a lowland area. *J. Soils Sediments* **2016**, *16*, 280–293. [CrossRef]
56. Lizaga, I.; Quijano, L.; Palazón, L.; Gaspar, L.; Navas, A. Enhancing connectivity index to assess the effects of land use changes in a Mediterranean catchment. *Land Degrad. Dev.* **2018**, *29*, 663–675. [CrossRef]
57. Persichillo, M.; Bordoni, M.; Cavalli, M.; Crema, S.; Meisina, C. The role of human activities on sediment connectivity of shallow landslides. *Catena* **2018**, *160*, 261–274. [CrossRef]
58. López-Vicente, M.; Poesen, J.; Navas, A.; Gaspar, L. Predicting runoff and sediment connectivity and soil erosion by water for different land use scenarios in the Spanish Pre-Pyrenees. *Catena* **2013**, *102*, 62–73. [CrossRef]
59. Morgan, R.P.C. A simple approach to soil loss prediction: A revised Morgan–Morgan–Finney model. *Catena* **2001**, *44*, 305–322. [CrossRef]
60. López-Vicente, M.; Navas, A. Routing runoff and soil particles in a distributed model with GIS: Implications for soil protection in mountain agricultural landscapes. *Land Degrad. Dev.* **2010**, *21*, 100–109. [CrossRef]
61. Roetzel, R.; Fuchs, G. *Geologische Karte der Republik Österreich, 1:50 000—8 Geras*; Geologische Bundesanstalt: Vienna, Austria, 2001.
62. IUSS Working Group WRB. *World Reference Base for Soil Resources 2014*; World Soil Resources Reports 106; Update 2015; FAO: Rome, Italy, 2015.
63. Laflen, J.M.; Lane, L.J.; Foster, G.R. WEPP: A new generation of erosion prediction technology. *J. Soil Water Conserv.* **1991**, *46*, 34–38.
64. Grønsten, H.; Lundekvam, H. Prediction of surface runoff and soil loss in southeastern Norway using the WEPP hillslope model. *Soil Tillage Res.* **2006**, *85*, 186–199. [CrossRef]
65. Singh, B.; Goel, R. Chapter 16—Shear strength of rock masses in slopes. In *Engineering Rock Mass Classification*; Singh, B., Goel, R., Eds.; Butterworth-Heinemann: Boston, MA, USA, 2011; pp. 205–210.
66. Mahmoodabadi, M.; Cerdà, A. WEPP calibration for improved predictions of interrill erosion in semi-arid to arid environments. *Geoderma* **2013**, *204*, 75–83. [CrossRef]
67. Brooks, E.S.; Dobre, M.; Elliot, W.J.; Wu, J.Q.; Boll, J. Watershed-scale evaluation of the Water Erosion Prediction Project (WEPP) model in the Lake Tahoe basin. *J. Hydrol.* **2016**, *533*, 389–402. [CrossRef]

68. Gould, G.K.; Liu, M.; Barber, M.E.; Cherkauer, K.A.; Robichaud, P.R.; Adam, J.C. The effects of climate change and extreme wildfire events on runoff erosion over a mountain watershed. *J. Hydrol.* **2016**, *536*, 74–91. [CrossRef]
69. Mirzaee, S.; Ghorbani-Dashtaki, S.; Mohammadi, J.; Asadzadeh, F.; Kerry, R. Modeling WEPP erodibility parameters in calcareous soils in northwest Iran. *Ecol. Indic.* **2017**, *74*, 302–310. [CrossRef]
70. Flanagan, D.C.; Frankenberger, J.R.; Cochrane, T.A.; Renschler, C.S.; Elliot, W.J. Geospatial application of the water erosion prediction project (WEPP) model. *Trans. ASABE* **2013**, *56*, 591–601. [CrossRef]
71. Nicks, A.D.; Gander, G.A. CLIGEN: A weather generator for climate inputs to water resource and other models. In Proceedings of the Fifth International Conference Computer Agriculture, Orlando, FL, USA, 6–9 February 1994; pp. 903–909.
72. Zhang, X.J.; Wang, Z. Interrill soil erosion processes on steep slopes. *J. Hydrol.* **2017**, *548*, 652–664. [CrossRef]
73. Muneer, T. *Solar Radiation and Daylight Models*; Routledge: London, UK, 2004; 392p.
74. McCullough, M.C.; Eisenhauer, D.E.; Dosskey, M. Modeling runoff and sediment yield from a terraced watershed using WEPP. In *USDA Forest Service*; USDA: Lincoln, NE, USA, 2008.
75. Donahue, R.L.; Miller, R.W.; Shickluna, J.C. *Soils: An Introduction to Soils and Plant Growth*; Prentice-Hall, Inc.: Englewood Cliffs, NJ, USA, 1983; 667p.
76. Xiong, H.; Goergen, J.; Yasumiishi, M.; Renschler, C.S. GeoWEPP for ArcGIS 10.x Version Overview Manual. Available online: http://geowepp.geog.buffalo.edu/wp-content/uploads/2014/01/GeoWEPP_ArcGIS10_Overview.pdf (accessed on 4 October 2019).
77. Pandey, A.; Chowdary, V.; Mal, B.; Billib, M. Runoff and sediment yield modeling from a small agricultural watershed in India using the WEPP model. *J. Hydrol.* **2008**, *348*, 305–319. [CrossRef]
78. Baffaut, C.; Nearing, M.A.; Govers, G. Statistical distributions of soil loss from runoff plots and WEPP model simulations. *Soil Sci. Soc. Am. J.* **1998**, *62*, 756–763. [CrossRef]
79. Okoba, B.O.; Sterk, G. Farmers' identification of erosion indicators and related erosion damage in the Central Highlands of Kenya. *Catena* **2006**, *65*, 292–301. [CrossRef]
80. Crema, S.; Schenato, L.; Goldin, B.; Marchi, L.; Cavalli, M. Toward the development of a stand-alone application for the assessment of sediment connectivity. *Rend. Online Soc. Geol. Ital.* **2015**, *34*, 58–61. [CrossRef]
81. Cavalli, M.; Crema, S.; Marchi, L. *Guidelines on the Sediment Connectivity ArcGis Toolbox and Stand-Alone Application*; CNR-IRPI: Padova, Italy, 2014.
82. Bakker, M.M.; Govers, G.; van Doorn, A.; Quetier, F.; Chouvardas, D.; Rounsevell, M. The response of soil erosion and sediment export to land-use change in four areas of Europe: The importance of landscape pattern. *Geomorphology* **2008**, *98*, 213–226. [CrossRef]
83. Panagos, P.; Borrelli, P.; Meusburger, K.; Alewell, C.; Lugato, E.; Montanarella, L. Estimating the soil erosion cover-management factor at the European scale. *Land Use Policy* **2015**, *48*, 38–50. [CrossRef]
84. Jenks, G.F. The Data Model Concept in Statistical Mapping. *Int. Yearb. Cartogr.* **1967**, *7*, 186–190.
85. Garbrecht, J.; Martz, L.W. The assignment of drainage direction over flat surfaces in raster digital elevation models. *J. Hydrol.* **1997**, *193*, 204–213. [CrossRef]
86. Haselberger, S. Modeling Human Induced Soil Erosion Hot Spots in a Medium-Sized Agricultural Catchment in the Thayatal Region, Lower Austria. Ph.D. Thesis, University of Vienna, Vienna, Austria, 2017.
87. Klik, A. Bodenerosion durch Wasser. *Ländlicher Raum* **2004**, *6*, 1–11.
88. De Vente, J.; Poesen, J.; Verstraeten, G.; Govers, G.; Vanmaercke, M.; Van Rompaey, A.; Arabkhedri, M.; Boix-Fayos, C. Predicting soil erosion and sediment yield at regional scales: Where do we stand? *Earth-Sci. Rev.* **2013**, *127*, 16–29. [CrossRef]
89. López-Vicente, M.; Álvarez, S. Influence of DEM resolution on modelling hydrological connectivity in a complex agricultural catchment with woody crops. *Earth Surf. Process. Landf.* **2018**, *43*, 1403–1415. [CrossRef]
90. Poeppl, R.E.; Parsons, A. The geomorphic cell: A basis for studying connectivity. *Earth Surf. Process. Landf.* **2018**, *43*, 1155–1159. [CrossRef]
91. Lemma, H.; Frankl, A.; van Griensven, A.; Poesen, J.; Adgo, E.; Nyssen, J. Identifying erosion hotspots in Lake Tana Basin from a multi-site SWAT validation: Opportunity for land managers. *Land Degrad. Dev.* **2019**, *30*, 1449–1467. [CrossRef]
92. Zhang, Z.; Sheng, L.; Yang, J.; Chen, X.; Kong, L.; Wagan, B. Effects of Land Use and Slope Gradient on Soil Erosion in a Red Soil Hilly Watershed of Southern China. *Sustainability* **2015**, *7*, 14309–14325. [CrossRef]

93. Fryirs, K.A.; Brierley, G.J.; Preston, N.J.; Spencer, J. Catchment-scale (dis)connectivity in sediment flux in the upper Hunter catchment, New South Wales, Australia. *Geomorphology* **2007**, *84*, 297–316. [CrossRef]
94. Kalantari, Z.; Cavalli, M.; Cantone, C.; Crema, S.; Destouni, G. Flood probability quantification for road infrastructure: Data-driven spatial-statistical approach and case study applications. *Sci. Total Environ.* **2017**, *581*, 386–398. [CrossRef]